How to cite: *Angew. Chem. Int. Ed.* **2023**, *62*, e202309928
doi.org/10.1002/anie.202309928

Sensors

Detection of Per- and Polyfluoroalkyl Substances (PFAS) by Interrupted Energy Transfer

*Alberto Concellón and Timothy M. Swager**

Abstract: The ubiquitous presence of per- and polyfluoroalkyl substances (PFAS) in aqueous environments has aroused societal concern. Nonetheless, effective sensing technologies for continuous monitoring of PFAS within water distribution infrastructures currently do not exist. Herein, we describe a ratiometric sensing approach to selectively detect aqueous perfluorooctanoic acid (PFOA) and perfluorooctane sulfonate (PFOS) at concentrations of $\mu g \cdot L^{-1}$. Our method relies on the excitonic transport in a highly fluorinated poly(p-phenylene ethynylene) to amplify a ratiometric emission signal modulated by an embedded fluorinated squaraine dye. The electronic coupling between the polymer and dye occurs through overlap of π-orbitals and is designed such that energy transfer is dominated by an electron-exchange (Dexter) mechanism. Exposure to aqueous solutions of PFAS perturbs the orbital interactions between the squaraine dye and the polymer backbone, thereby diminishing the efficiency of the energy transfer and producing a "polymer-ON/dye-OFF" response. These polymer/dye combinations were evaluated in spin-coated films and polymer nanoparticles and were able to selectively detect PFAS at concentrations of ca. 150 ppb and ca. 50 ppb, respectively. Both polymer films and nanoparticles are not affected by the type of water, and similar responses to PFAS were found in milliQ and well water.

Per- and polyfluoroalkyl substances (PFAS) are omnipresent in our daily life and are widely used across multiple industries. The tendency of PFAS to accumulate over time in the environment, and the increasing evidence of their detrimental health effects in living systems, have aroused major societal concerns about their use, mitigation, and detection.[1] In particular PFAS can accumulate in humans even with exposure at ultra-trace levels, which have resulted in US Environmental Protection Agency (EPA) legally enforceable levels of 4 $ng \cdot L^{-1}$ (ppt) for perfluorooctanoic acid (PFOA) and 4 $ng \cdot L^{-1}$ for perfluorooctane sulfonate (PFOS) in drinking water.[2] These ultra-low concentrations, as well as the complexity of real water samples, make PFAS detection extremely challenging. Current EPA detection methods rely on solid-phase extraction from water and subsequent analysis by liquid chromatography-tandem mass spectroscopy.[3][4] Despite the fact that these methods provide the required sensibility and accuracy, they are time-consuming, cost-prohibitive, and required complex specialized equipment with well-trained personnel. Technologies capable of continuous monitoring of PFAS through distributed water infrastructures currently do not exist. Therefore, current investigations are focused on developing quick, portable, low-cost PFAS sensing devices, such as fluorescent and optical sensors, or electrochemical sensors.[5] In particular, fluorescent sensors are the most widely employed as a consequence of their versatility, but they have PFAS detection limits around the ppm and ppb levels, with few examples in the low-ppb range.[6]

We report herein a PFAS detection mechanism that is based on energy transfer (ET) interruption, in which a fluorescent conjugated polymer acts as a light-harvesting unit (donor) to amplify the emission from a dye (acceptor). There are two mechanisms for ET in these systems; Förster resonance energy transfer (FRET),[7] and electron-exchange pathways formulated by Dexter.[8] The former can proceed over 10s of nanometers through dipole-dipole interactions and requires spectral overlap between the donor's emission and the acceptor's absorption. The latter requires π–π orbital overlap between the conjugated polymer donor and the dye acceptor to enable the necessary electronic coupling. A key consideration is that electron-exchange pathways are extremely sensitive to intermolecular distance changes of only few angstroms. In this context, our group previously described a selective sensor scheme to detect cyclic ketones via exchange-based ET, wherein small binding interactions between the analyte and a dye cause small movements within the polymer pores (0.5–2 Å).[9] It was found that analyte binding reduces π-orbital overlapping, leading to a decrease of the dye emission and to an increase in the polymer emission.

Herein, we have designed a selective ratiometric sensing approach to detect PFAS in aqueous environments through

[*] Dr. A. Concellón, Prof. Dr. T. M. Swager
Department of Chemistry
Massachusetts Institute of Technology
77 Massachusetts Avenue, Cambridge, Massachusetts 02139 (United States)
E-mail: tswager@mit.edu
Dr. A. Concellón
Present address: Instituto de Nanociencia y Materiales de Aragón (INMA), CSIC-University of Zaragoza, 50009 Zaragoza (Spain)

interrupted exchange-based ET. Our method relies on the ability of a poly(*p*-phenylene ethynylene) containing fluorinated alkane side groups to participate in energy transfer to an embedded fluorinated fluorophore (Figure 1). The fluorinated side-chains serve to partition PFAS into polymers,[10] and the rigid pentiptycene repeating units introduce molecular-level porosity that facilitates PFAS diffusion into the solid polymers and galleries in which the guest dyes localize. Exposure of these composites to aqueous solutions of PFAS produces a small displacement of the dye from the polymer backbone, thereby diminishing the efficiency of the ET and producing a ratiometric fluorescent response ("polymer-ON/dye-OFF"). Specifically, we synthesized two polymers, **PPE** and **^{F}PPE**, wherein **^{F}PPE** polymer possesses a particularly high fluorine content (61 wt. %) in comparison to **PPE** (43 wt. %), which potentially increases PFAS affinity for the polymer. As for the acceptors, we selected three fluorinated dyes, a squaraine (**F-Sq**), an oxazine (**F-Ox**) and a perylene bisimide (**F-PBI**) derivatives, which have negligible spectral overlap with the light-harvesting **PPE** and **^{F}PPE** so that polymer to dye ET may proceed dominantly through an electron exchange mechanism.[11]

The fluorous-squaraine (**F-Sq**), fluorous-oxazine (**F-Ox**), and fluorous-perylene bisimide (**F-FBI**) were synthesized following previously reported procedures.[11] The conjugated polymers, **PPE** and **^{F}PPE**, were synthesized by palladium-catalyzed Sonogashira polymerization between diethylnyl [2.2.2] bridged bicyclic monomers, and a diiodide in benzotrifluoride/diisopropylamine (3:2) (Scheme S1). Both polymers were purified by precipitation in methanol, followed by repeatedly washings with hot methanol and acetone. The average molar mass and polydispersity index of **PPE** were estimated by gel permeation chromatography (GPC) in THF solution using polystyrene standards. Nonetheless, the exclusive solubility of **^{F}PPE** in fluorinated solvents prevented the determination of its molar mass by GPC. Therefore, we made use of dynamic light scattering (DLS) to estimate the length distribution of **^{F}PPE**. DLS measurements in benzotrifluoride solution showed a 18.7 nm radius of gyration, which is similar to the persistence length of high-molecular weight poly(*p*-phenylene ethynylene)s.[12]

To optimize the sensor formulations, several weight ratios of the dye (**F-Sq**, **F-Ox**, or **F-PBI**) were combined with the polymer (**PPE**, or **^{F}PPE**). Briefly, the polymer and the dye were dissolved in benzotrifluoride, followed by spin-casting onto clean glass substrates. The fluorescence spectra of these thin films showed that **F-Ox** and **F-PBI** displayed a negligible ET with only very weak emission signals upon excitation of **PPE** or **^{F}PPE** (Figure S1). In contrast **F-Sq** undergoes facile energy transfer with both conjugated polymers (Figure 2a). Given the negligible spectra overlap

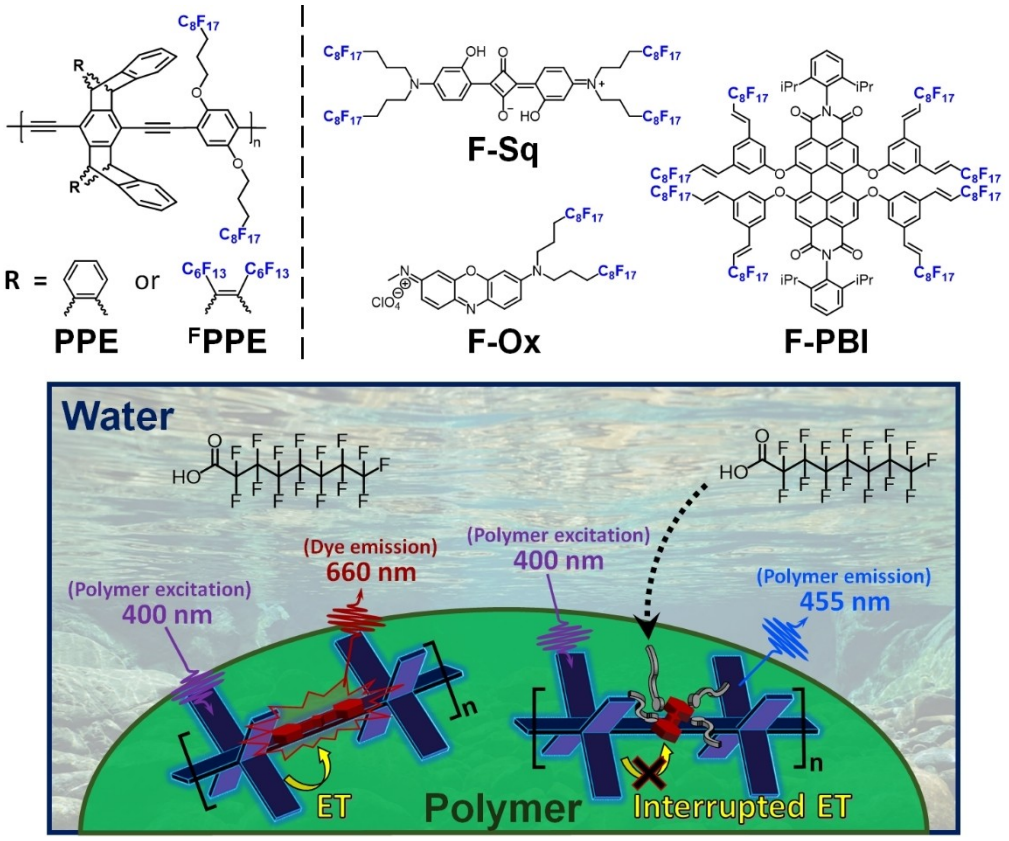

Figure 1. Chemical structure of the fluorous poly(*p*-phenylene ethynylenes) and fluorous dyes. Conceptual scheme of the mechanism for the detection of PFAS in water: PFOA diffusion from water into the polymer disrupts π–π interactions between the dye and the conjugated polymer, interrupting the electron-exchange-based ET.

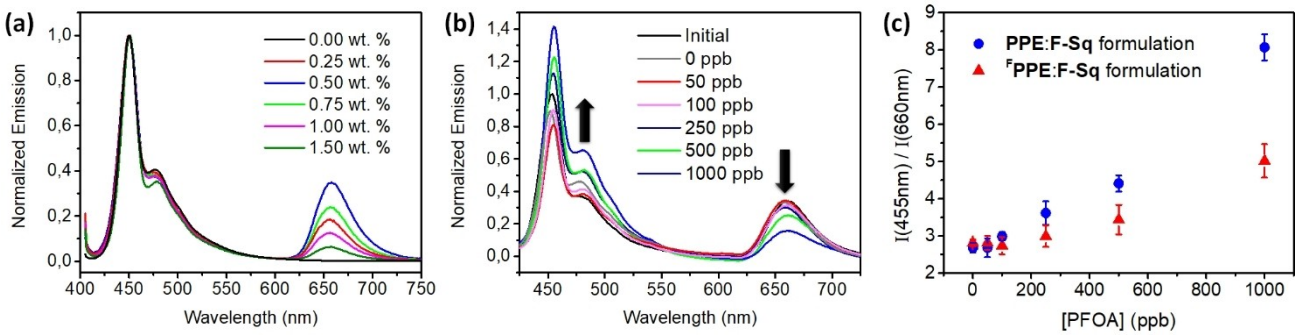

Figure 2. **(a)** Thin-film fluorescence spectra of **PPE**:**F-Sq** as a function of dye loading. **(b)** Thin-film fluorescence spectra of **PPE**:**F-Sq** upon exposure to aqueous solutions of PFOA. **(c)** Ratio of thin-film fluorescence intensity at 455 nm to that at 660 nm as a function of PFOA concentration in milliQ water (average values of three different films, errors bars represent standard deviations).

between **PPE**/**^{F}PPE** and **F-Sq** (Figure S1a), the observed ET process is dominated by an exchange mechanism, in which conceptually there are electron exchanges from the excited polymer to the ground state squaraine dye to create an excited **F-Sq***. In this scheme it is of critical importance the formation of efficient π–π interactions between the embedded dye and the polymer backbone. Thus, the size and aspect ratio of the **F-Sq** chromophore likely ensures a close packing with the polymer backbone. Alternatively, the molecular geometry, molecular orbitals distribution, and size of **F-Ox** and **F-PBI** appear to prevent strong π–π interactions for very limited exchange-based ET. As a result, all subsequent sensing studies are focused on mixtures containing **F-Sq**. We found that a dye loading of 0.5 wt. % gave the optimal balance between polymer emission and amplification of **F-Sq** emission, whereas higher dye loadings showed a decrease of the squaraine emission likely due to self-aggregation (Figure 2a).

PFAS detection is based on an interruption of the ET between the **PPE**/**^{F}PPE** polymer and **F-Sq**. Given the strong tendency of perfluoralkanes to colocalize, we expect that the equilibrium geometry of the **F-Sq**:**PPE**/**^{F}PPE** complex has maximized these interactions. Absorption of additional PFAS molecules in effect drives a wedge between the two groups and disrupts the polymer-dye π–π interactions responsible for the exchange-based ET. The sensor response time is likely dominated the time needed for PFAS molecules to diffuse from water to the fluorophilic polymer film.[10] Accordingly we used an exposure time of one hour to perform all our sensing experiments to ensure appropriate PFAS diffusion into the polymer films.[6c] Exposure of such thin films (30 to 50 Å thick) to aqueous solutions of PFOA resulted in a decrease of **F-Sq** emission ("dye-OFF") and in an increase of **PPE**/**^{F}PPE** emission ("polymer-ON") (Figure 2b). Despite the higher fluorine content of **^{F}PPE** polymer, this sensor formulation showed lower fluorescence response than that of **PPE** polymer. The higher fluorous nature of **^{F}PPE** and the poor wettability of its films probably reduces the diffusion of PFOA molecules from water into the polymer. Additionally, the extra fluoroalkane side groups of **^{F}PPE** may result in PFOA binding in ways that doesn't impact the dye-polymer interactions. The limits of PFOA detection were calculated to be 126 ppb for **PPE**:**F-Sq** formulation, and 282 ppb for **^{F}PPE**:**F-Sq**. Interestingly, the **PPE**:**F-Sq** films do not exhibit the same fluorescence response when exposed to aqueous solutions of simple octanoic acid (Figure S2), thereby demonstrating that the fluorinated segments within the conjugated polymers selectively bind and respond to PFOA. To rule out direct interactions between the **PPE** polymer backbone (without **F-Sq**) and PFAS, we conducted a study on **PPE**'s emission response to PFOA. Nevertheless, no change in emission was observed when **PPE** films were exposed to PFOA (see Figure S3). This indicates that the distinct PFAS response of our polymer sensor results from an interruption in exchange-based energy transfer between **PPE** and **F-Sq**.

The detection mechanism of our polymer sensors relies on the adsorption of perfluorinated molecules by highly fluorinated polymers, and this triggers ET interruption between the polymer backbone and the dye. Thus, we wondered if **PPE**:**F-Sq** formulations could have general utility to sense other PFAS molecules, such as PFOS. As shown in Figure 3, we observed minor deviations in the fluorescence response after exposing **PPE**:**F-Sq** films to several concentrations of PFOS, and also the same detection limits within the margin of error (126 ppb for PFOA and 141 ppb for PFOS). We considered that the ET interruption-based sensing mechanism may be susceptible to several interferences that are commonly found in complex aqueous matrixes (e.g., ground water). To evaluate the robustness of our sensors, we decided to evaluate their performance by using a realistic aqueous matrix from a well in Central Vermont. Nonetheless, we observed similar fluorescence responses to PFOA and PFOS, demonstrating that our polymer sensors are not affected by the type of water **(**Figure 3).

The observed response to PFAS is likely to be highly dependent on the polymer/water interfacial area that affects the time needed for PFAS to diffuse from water into polymer film. Therefore, we decided to use conjugated polymer nanoparticle (CPdots) dispersions in water with the intent to increase the polymer/water interfacial area and accelerate PFAS partition into polymers. We prepared CPdots aqueous dispersions by a reprecipitation method,

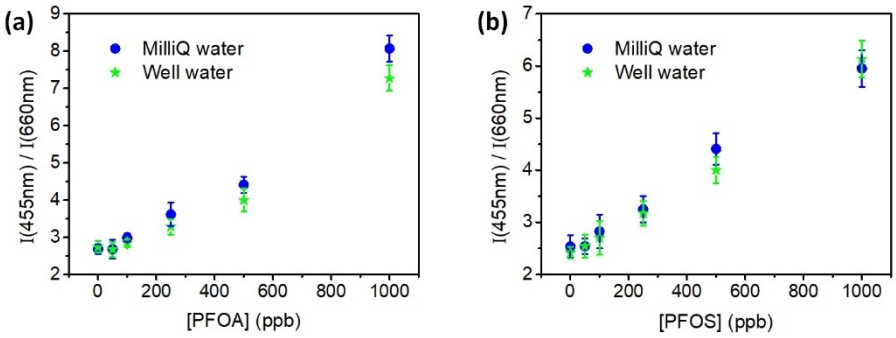

Figure 3. Ratio of thin-film fluorescence intensity at 455 nm to that at 660 nm as a function of **(a)** PFOA or **(b)** PFOS concentration in milliQ water and well water (average values of three different films, errors bars represent standard deviations).

wherein a dilute THF solution of the polymer/dye mixture (0.01 $mg \cdot mL^{-1}$, 2 mL) was quickly added to water (8 mL) under sonication, followed by THF evaporation under reduced pressure. The obtained aqueous dispersions of CPdots were optically clear and were stable over 1 month with no evidence of precipitation. **^{F}PPE** polymer was only soluble in fluorinated solvents, thereby preventing the preparation of CPdots since it requires water-soluble organic solvents, such as THF. As a result, CPdots sensing studies were exclusively focused on **PPE**:**F-Sq** formulations. The average size of CPdots was determined by DLS, obtaining monomodal size distributions (PDI < 0.20) with mean hydrodynamic diameters of 88 nm (Figure 4a). The morphology of the CPdots was investigated by transmission electron microscopy (TEM) (Figure 4b). TEM images evidence the presence of spherical nanoparticles that appear to aggregate forming an interconnected network. The formation of such interconnected networks was previously observed for CPdots,[13] and is related to the high hydrophobicity of our fluorinated polymer that causes aggregation with water evaporation.

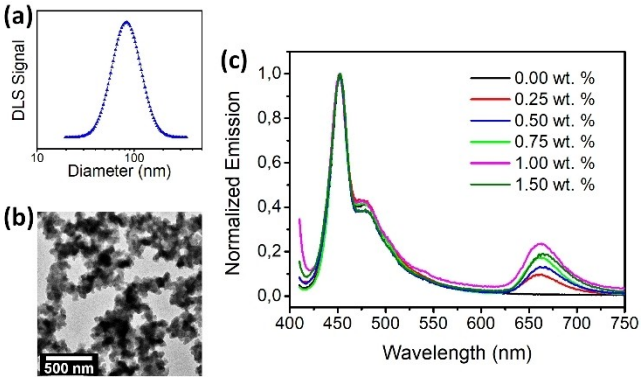

Figure 4. **(a)** DLS measurements of water dispersions of **PPE**:**F-Sq** CPdots. **(b)** TEM image of **PPE**:**F-Sq** CPdots. **(c)** Fluorescence spectra of **PPE**:**F-Sq** CPdots as a function of dye loading.

The fluorescence spectra of **PPE**:**F-Sq** CPdots were very similar to the spectra acquired in thin film form (Figure 4c). This result evidences that **F-Sq** acceptor also undergoes facile energy transfer when is colocalized in CPdots of **PPE** polymer, thereby demonstrating a robust assembly process between the dye and polymer. In this case, a dye loading of 1.0 wt. % was found to give the optimal polymer/dye emission balance. The fluorescence spectra of the CPdots were recorded after one hour incubation with different concentrations of PFOA in milliQ and well water. In the same manner as thin film experiments, PFOA exposure resulted in a ratiometric "polymer-ON/dye-OFF" response that was not affected by the type of water (Figure 5a). CPdots-based sensors were also able to detect PFOS in addition to PFOA (Figure 5b). These results confirmed that PFAS molecules are able to diffuse into CPdots and disrupt

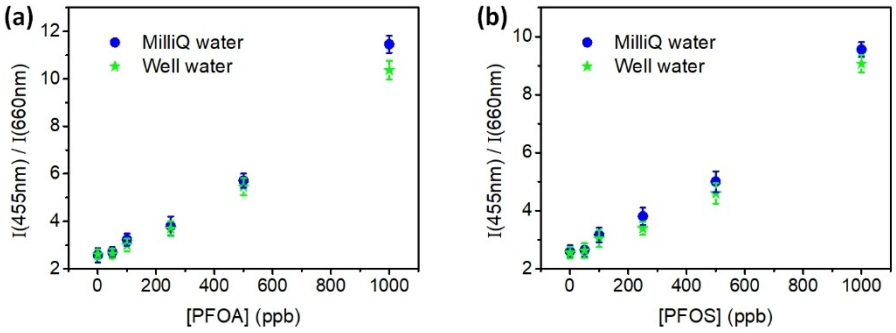

Figure 5. Ratio of CPdots fluorescence intensity at 455 nm to that at 660 nm as a function of **(a)** PFOA or **(b)** PFOS concentration in milliQ water and well water (average values of three different CPdots dispersions, errors bars represent standard deviations).

π–π interactions between **F-Sq** and **PPE**, interrupting their ET. We calculated a detection limit of 59 ppb for PFOA, and 68 ppb for PFOS. Comparison of thin film and CPdots limits of detection shows that CPdots aqueous dispersions are more sensitive than thin films, evidencing the impact of a higher surface area in our polymer sensors.

Our most effective system (i.e., **PPE**:**F-Sq** in CPdot form) can detect PFOA and PFOS concentrations of 59 ppb and 68 ppb, respectively. We have recently reported an exceptionally sensitive optical sensor for PFAS, achieving remarkable detection limits of 0.08 ppb for PFOA and 0.35 ppb for PFOS.[6c] These polymer sensors exhibit an exclusive response to acidic PFAS molecules, owing to the presence of pyridine moieties within the polymer structure. The protonation of these pyridines by PFAS leads to the formation of lower-energy pyridinium traps for excitons, resulting in a red shift of the emission spectra. In contrast, our current study introduces a novel sensing approach based on an interrupted exchange-based ET, offering the potential to detect a broader range of PFAS molecules, including acidic, basic, and neutral species. Although the achieved detection limits do not match the exceptional sensitivity of our previous work, they do position our sensor scheme among the most sensitive optical sensors for PFAS reported to date.

In conclusion, we have developed a new fluorescent sensing approach to selectively detect PFOA and PFOS in aqueous environments at concentrations of $\mu g \cdot L^{-1}$. Our approach is based on the light-harvesting ability of poly(*p*-phenylene ethynylene)s to amplify the emission from an embedded dye, as well as the strong distance dependance of the electron exchange-based energy transfer process. To facilitate PFAS partition from water into polymers, we designed highly fluorinated polymers and dyes as the sensing elements. Exposure to aqueous solutions of PFAS produces a small displacement of the dye from the polymer backbone, diminishing the efficiency of the energy transfer and producing a ratiometric fluorescent response ("polymer-ON/dye-OFF"). These polymer/dye combinations were evaluated as spin-coated films and as polymer nanoparticles, and were able to selectively detect PFAS at concentrations of ~150 ppb and ~50 ppb, respectively. Both polymer films and nanoparticles were not affected by the type of water, and similar responses to PFAS were found in milliQ and well water. While additional refinements are needed to meet the legally enforceable limits established by the US EPA (4 ppt for PFOA and PFOS, individually), these results illustrate an effective sensing method for the detection of aqueous PFAS without relying on complex specialized facilities. This approach can be applied for on-site PFAS detection in heavily contaminated regions or after preconcentrating water samples through solid-phase extraction. Investigations to discriminate short- and long-chain PFAS, and to detect PFAS with different functionality are currently underway in our laboratory.

Acknowledgements

We are grateful for support from support from Xylem Corporation and the MIT Jameel Water and Food Security Center. We also thank our colleagues Jessica C. Beard for helpful discussions, Kosuke Yoshinaga for the fluorous perylene bisimide (**F-FBI**), and Weize Yuan for TEM.

Conflict of Interest

A provisional patent has been filed.

Data Availability Statement

The data that support the findings of this study are available in the supplementary material of this article.

Keywords: Conjugated Polymers · Energy Transfer · Fluorous Polymers · PFAS · Sensors

[1] a) K. Kannan, *Environ. Chem.* **2011**, *8*, 333–338; b) R. C. Buck, J. Franklin, U. Berger, J. M. Conder, I. T. Cousins, P. de Voogt, A. A. Jensen, K. Kannan, S. A. Mabury, S. P. van Leeuwen, *Integr. Environ. Assess. Manage.* **2011**, *7*, 513–541; c) D. O'Hagan, *Chem. Soc. Rev.* **2008**, *37*, 308–319; d) E. M. Bell, S. De Guise, J. R. McCutcheon, Y. Lei, M. Levin, B. Li, J. F. Rusling, D. A. Lawrence, J. M. Cavallari, C. O'Connell, B. Javidi, X. Wang, H. Ryu, *Sci. Total Environ.* **2021**, *780*, 146399; e) J. M. Graber, C. Alexander, R. J. Laumbach, K. Black, P. O. Strickland, P. G. Georgopoulos, E. G. Marshall, D. G. Shendell, D. Alderson, Z. Mi, M. Mascari, C. P. Weisel, *J. Expo. Sci. Environ. Epidemiol.* **2019**, *29*, 172–182; f) E. M. Sunderland, X. C. Hu, C. Dassuncao, A. K. Tokranov, C. C. Wagner, J. G. Allen, *J. Expo. Sci. Environ. Epidemiol.* **2019**, *29*, 131–147; g) V. Barry, A. Winquist, K. Steenland, *Environ. Health Perspect.* **2013**, *121*, 1313–1318; h) F. Suja, B. K. Pramanik, S. M. Zain, *Water Sci. Technol.* **2009**, *60*, 1533–1544.

[2] Fact Sheet: EPA's Proposal to Limit PFAS in Drinking Water; United States Environmental Protection Agency: Washington, D.C, 2023.

[3] Method 533: Determination of Per- and Polyfluoroalkyl Substances in Drinking Water by Isotope Dilution Anion Exchange Solid Phase Extraction and Liquid Chromatography/Tandem Mass Spectrometry. United States Environmental Protection Agency, Washington, D.C, 2019.

[4] Method 537.1 Determination of Selected Per- and Polyflourinated Alkyl Substances in Drinking Water by Solid Phase Extraction and Liquid Chromatography/Tandem Mass Spectrometry (LC/MS/MS). United States Environmental Protection Agency, Washington, D.C, 2020.

[5] a) K. L. Rodriguez, J.-H. Hwang, A. R. Esfahani, A. H. M. A. Sadmani, W. H. Lee, *Micromachines* **2020**, *11*, 667; b) Y. Wang, S. B. Darling, J. Chen, *ACS Appl. Mater. Interfaces* **2021**, *13*, 60789–60814; c) S. Garg, P. Kumar, G. W. Greene, V. Mishra, D. Avisar, R. S. Sharma, L. F. Dumée, *J. Environ. Manage.* **2022**, *308*, 114655; d) M. Al Amin, Z. Sobhani, Y. Liu, R. Dharmaraja, S. Chadalavada, R. Naidu, J. M. Chalker, C. Fang, *Environ. Technol. Innov.* **2020**, *19*, 100879; e) V. Trinh, C. S. Malloy, T. J. Durkin, A. Gadh, S. Savagatrup, *ACS Sens.* **2022**, *7*, 1514–1523; f) S. P. Sahu, S. Kole, C. G. Arges, M. R.

Gartia, *ACS Omega* **2022**, *7*, 5001–5007; g) F. Faiz, G. Baxter, S. Collins, F. Sidiroglou, M. Cran, *Sens. Actuators B* **2020**, *312*, 128006; h) R. B. Clark, J. E. Dick, *ACS Sens.* **2020**, *5*, 3591–3598; i) R. Ranaweera, C. Ghafari, L. Luo, *Anal. Chem.* **2019**, *91*, 7744–7748; j) C. Fang, J. Wu, Z. Sobhani, M. A. Amin, Y. Tang, *Anal. Methods* **2019**, *11*, 163–170.

[6] a) Z. Zheng, H. Yu, W.-C. Geng, X.-Y. Hu, Y.-Y. Wang, Z. Li, Y. Wang, D.-S. Guo, *Nat. Commun.* **2019**, *10*, 5762; b) E. E. Harrison, M. L. Waters, *Chem. Sci.* **2023**, *14*, 928–936; c) A. Concellón, J. Castro-Esteban, T. M. Swager, *J. Am. Chem. Soc.* **2023**, *145*, 11420–11430.

[7] T. Förster, *Ann. Phys.* **1948**, *437*, 55–75.

[8] D. L. Dexter, *J. Chem. Phys.* **1953**, *21*, 836–850.

[9] J. R. Cox, P. Müller, T. M. Swager, *J. Am. Chem. Soc.* **2011**, *133*, 12910–12913.

[10] a) R. Wang, Z.-W. Lin, M. J. Klemes, M. Ateia, B. Trang, J. Wang, C. Ching, D. E. Helbling, W. R. Dichtel, *ACS Cent. Sci.* **2022**, *8*, 663–669; b) C. Wu, M. J. Klemes, B. Trang, W. R. Dichtel, D. E. Helbling, *Water Res.* **2020**, *182*, 115950; c) L. Xiao, Y. Ling, A. Alsbaiee, C. Li, D. E. Helbling, W. R. Dichtel, *J. Am. Chem. Soc.* **2017**, *139*, 7689–7692.

[11] a) K. Yoshinaga, T. M. Swager, *Synlett* **2018**, *29*, 2509–2514; b) E. M. Sletten, T. M. Swager, *J. Am. Chem. Soc.* **2014**, *136*, 13574–13577.

[12] a) J. Lim, T. M. Swager, *Angew. Chem. Int. Ed.* **2010**, *49*, 7486–7488; b) P. M. Cotts, T. M. Swager, Q. Zhou, *Macromolecules* **1996**, *29*, 7323–7328.

[13] C. Szymanski, C. Wu, J. Hooper, M. A. Salazar, A. Perdomo, A. Dukes, J. McNeill, *J. Phys. Chem. B* **2005**, *109*, 8543–8546.

Manuscript received: August 28, 2023
Accepted manuscript online: October 5, 2023
Version of record online: October 19, 2023